

1 Rose and lavender industrial by-products application for adsorption of Acid
2
3 orange 7 from aqueous solution
4
5
6
7

8 Gergana Marovska¹, Mariya Dushkova², Galena Angelova³, Mariya Brazkova³, Hendrik
9
10 Brink⁴, Nils Haneklaus^{5,6}, Nikolay Menkov², Anton Slavov^{1*}
11
12
13
14

15 ¹Department of Organic Chemistry, Technological Faculty, University of Food Technologies,
16
17 26 Maritsa Blvd., Plovdiv 4002, Bulgaria. e-mails: Gergana Marovska (ORCID: [0000-0002-
18 2687-3366](https://orcid.org/0000-0002-2687-3366)): gerii_vlaseva@abv.bg; Anton Slavov (ORCID [0000-0002-2699-5929](https://orcid.org/0000-0002-2699-5929)):
19
20 antons@uni-plovdiv.net
21
22
23
24

25 ²Department of Process Engineering, Technical Faculty, University of Food Technologies, 26
26
27 Maritsa Blvd., Plovdiv 4002, Bulgaria. e-mails: Nikolay Menkov (ORCID [0000-0002-8585-
28 6734](https://orcid.org/0000-0002-8585-6734)): nimenkov@yahoo.com; Mariya Dushkova (ORCID [0000-0002-4157-2684](https://orcid.org/0000-0002-4157-2684)):
29
30 maria_douchkova@yahoo.fr
31
32
33
34

35 ³Department of Biotechnology, University of Food Technologies, 26 Maritsa Blvd., 4002
36
37 Plovdiv, Bulgaria; e-mails: Galena Angelova (ORCID [0000-0003-1452-8116](https://orcid.org/0000-0003-1452-8116)):
38
39 g_angelova@uft-plovdiv.bg; Mariya Brazkova (ORCID [0000-0002-0184-9511](https://orcid.org/0000-0002-0184-9511)):
40
41 mbrazkova@uft-plovdiv.bg
42
43
44

45 ⁴Department of Chemical Engineering, Faculty of Engineering, Built Environment and
46
47 Information Technology, University of Pretoria, Pretoria 0002, South Africa; ORCID [0000-
48 0002-4699-6152](https://orcid.org/0000-0002-4699-6152); e-mail: deon.brink@up.ac.za
49
50
51

52 ⁵Td-Lab Sustainable Mineral Resources, University for Continuing Education Krems, Dr.-
53
54 Karl-Dorrek-Straße 30, 3500 Krems, Austria. ORCID [0000-0002-0673-0376](https://orcid.org/0000-0002-0673-0376); e-mail:
55
56 nils.haneklaus@donau-uni.ac.at
57
58

25 ⁶Institute of Chemical Technology, Technische Universität Bergakademie Freiberg, Leipziger
1
2
3
4
26 Straße 29, 09599 Freiberg, Germany. e-mail: nils.haneklaus@chemie.tu-freiberg.de

5
6
7
8
9
10
11
12
13
14
15
16
17
18
19
20
21
22
23
24
25
26
27
28
29 *Corresponding author: Department of Organic Chemistry and Inorganic Chemistry,
30
31 Technological Faculty, University of Food Technologies, 26 Maritza Blvd., Plovdiv 4002,
32
33 Bulgaria. antons@uni-plovdiv.net, ORCID [0000-0002-2699-5929](https://orcid.org/0000-0002-2699-5929)

34
35
36
37
38
39
40
41
42
43
44
45
46
47
48
49
50
51
52
53
54
55
56
57
58
59
60
61
62
63
64
65
66
67
68
69
70
71
72
73
74
75
76
77
78
79
80
81
82
83
84
85
86
87
88
89
90
91
92
93
94
95
96
97
98
99
100
101
102
103
104
105
106
107
108
109
110
111
112
113
114
115
116
117
118
119
120
121
122
123
124
125
126
127
128
129
130
131
132
133
134
135
136
137
138
139
140
141
142
143
144
145
146
147
148
149
150
151
152
153
154
155
156
157
158
159
160
161
162
163
164
165
166
167
168
169
170
171
172
173
174
175
176
177
178
179
180
181
182
183
184
185
186
187
188
189
190
191
192
193
194
195
196
197
198
199
200
201
202
203
204
205
206
207
208
209
210
211
212
213
214
215
216
217
218
219
220
221
222
223
224
225
226
227
228
229
230
231
232
233
234
235
236
237
238
239
240
241
242
243
244
245
246
247
248
249
250
251
252
253
254
255
256
257
258
259
260
261
262
263
264
265
266
267
268
269
270
271
272
273
274
275
276
277
278
279
280
281
282
283
284
285
286
287
288
289
290
291
292
293
294
295
296
297
298
299
300
301
302
303
304
305
306
307
308
309
310
311
312
313
314
315
316
317
318
319
320
321
322
323
324
325
326
327
328
329
330
331
332
333
334
335
336
337
338
339
340
341
342
343
344
345
346
347
348
349
350
351
352
353
354
355
356
357
358
359
360
361
362
363
364
365
366
367
368
369
370
371
372
373
374
375
376
377
378
379
380
381
382
383
384
385
386
387
388
389
390
391
392
393
394
395
396
397
398
399
400
401
402
403
404
405
406
407
408
409
410
411
412
413
414
415
416
417
418
419
420
421
422
423
424
425
426
427
428
429
430
431
432
433
434
435
436
437
438
439
440
441
442
443
444
445
446
447
448
449
450
451
452
453
454
455
456
457
458
459
460
461
462
463
464
465
466
467
468
469
470
471
472
473
474
475
476
477
478
479
480
481
482
483
484
485
486
487
488
489
490
491
492
493
494
495
496
497
498
499
500
501
502
503
504
505
506
507
508
509
510
511
512
513
514
515
516
517
518
519
520
521
522
523
524
525
526
527
528
529
530
531
532
533
534
535
536
537
538
539
540
541
542
543
544
545
546
547
548
549
550
551
552
553
554
555
556
557
558
559
560
561
562
563
564
565
566
567
568
569
570
571
572
573
574
575
576
577
578
579
580
581
582
583
584
585
586
587
588
589
590
591
592
593
594
595
596
597
598
599
600
601
602
603
604
605
606
607
608
609
610
611
612
613
614
615
616
617
618
619
620
621
622
623
624
625
626
627
628
629
630
631
632
633
634
635
636
637
638
639
640
641
642
643
644
645
646
647
648
649
650
651
652
653
654
655
656
657
658
659
660
661
662
663
664
665
666
667
668
669
670
671
672
673
674
675
676
677
678
679
680
681
682
683
684
685
686
687
688
689
690
691
692
693
694
695
696
697
698
699
700
701
702
703
704
705
706
707
708
709
710
711
712
713
714
715
716
717
718
719
720
721
722
723
724
725
726
727
728
729
730
731
732
733
734
735
736
737
738
739
740
741
742
743
744
745
746
747
748
749
750
751
752
753
754
755
756
757
758
759
760
761
762
763
764
765
766
767
768
769
770
771
772
773
774
775
776
777
778
779
780
781
782
783
784
785
786
787
788
789
790
791
792
793
794
795
796
797
798
799
800
801
802
803
804
805
806
807
808
809
810
811
812
813
814
815
816
817
818
819
820
821
822
823
824
825
826
827
828
829
830
831
832
833
834
835
836
837
838
839
840
841
842
843
844
845
846
847
848
849
850
851
852
853
854
855
856
857
858
859
860
861
862
863
864
865
866
867
868
869
870
871
872
873
874
875
876
877
878
879
880
881
882
883
884
885
886
887
888
889
890
891
892
893
894
895
896
897
898
899
900
901
902
903
904
905
906
907
908
909
910
911
912
913
914
915
916
917
918
919
920
921
922
923
924
925
926
927
928
929
930
931
932
933
934
935
936
937
938
939
940
941
942
943
944
945
946
947
948
949
950
951
952
953
954
955
956
957
958
959
960
961
962
963
964
965
966
967
968
969
970
971
972
973
974
975
976
977
978
979
980
981
982
983
984
985
986
987
988
989
990
991
992
993
994
995
996
997
998
999
1000
1001
1002
1003
1004
1005
1006
1007
1008
1009
1010
1011
1012
1013
1014
1015
1016
1017
1018
1019
1020
1021
1022
1023
1024
1025
1026
1027
1028
1029
1030
1031
1032
1033
1034
1035
1036
1037
1038
1039
1040
1041
1042
1043
1044
1045
1046
1047
1048
1049
1050
1051
1052
1053
1054
1055
1056
1057
1058
1059
1060
1061
1062
1063
1064
1065
1066
1067
1068
1069
1070
1071
1072
1073
1074
1075
1076
1077
1078
1079
1080
1081
1082
1083
1084
1085
1086
1087
1088
1089
1090
1091
1092
1093
1094
1095
1096
1097
1098
1099
1100
1101
1102
1103
1104
1105
1106
1107
1108
1109
1110
1111
1112
1113
1114
1115
1116
1117
1118
1119
1120
1121
1122
1123
1124
1125
1126
1127
1128
1129
1130
1131
1132
1133
1134
1135
1136
1137
1138
1139
1140
1141
1142
1143
1144
1145
1146
1147
1148
1149
1150
1151
1152
1153
1154
1155
1156
1157
1158
1159
1160
1161
1162
1163
1164
1165
1166
1167
1168
1169
1170
1171
1172
1173
1174
1175
1176
1177
1178
1179
1180
1181
1182
1183
1184
1185
1186
1187
1188
1189
1190
1191
1192
1193
1194
1195
1196
1197
1198
1199
1200
1201
1202
1203
1204
1205
1206
1207
1208
1209
1210
1211
1212
1213
1214
1215
1216
1217
1218
1219
1220
1221
1222
1223
1224
1225
1226
1227
1228
1229
1230
1231
1232
1233
1234
1235
1236
1237
1238
1239
1240
1241
1242
1243
1244
1245
1246
1247
1248
1249
1250
1251
1252
1253
1254
1255
1256
1257
1258
1259
1260
1261
1262
1263
1264
1265
1266
1267
1268
1269
1270
1271
1272
1273
1274
1275
1276
1277
1278
1279
1280
1281
1282
1283
1284
1285
1286
1287
1288
1289
1290
1291
1292
1293
1294
1295
1296
1297
1298
1299
1300
1301
1302
1303
1304
1305
1306
1307
1308
1309
1310
1311
1312
1313
1314
1315
1316
1317
1318
1319
1320
1321
1322
1323
1324
1325
1326
1327
1328
1329
1330
1331
1332
1333
1334
1335
1336
1337
1338
1339
1340
1341
1342
1343
1344
1345
1346
1347
1348
1349
1350
1351
1352
1353
1354
1355
1356
1357
1358
1359
1360
1361
1362
1363
1364
1365
1366
1367
1368
1369
1370
1371
1372
1373
1374
1375
1376
1377
1378
1379
1380
1381
1382
1383
1384
1385
1386
1387
1388
1389
1390
1391
1392
1393
1394
1395
1396
1397
1398
1399
1400
1401
1402
1403
1404
1405
1406
1407
1408
1409
1410
1411
1412
1413
1414
1415
1416
1417
1418
1419
1420
1421
1422
1423
1424
1425
1426
1427
1428
1429
1430
1431
1432
1433
1434
1435
1436
1437
1438
1439
1440
1441
1442
1443
1444
1445
1446
1447
1448
1449
1450
1451
1452
1453
1454
1455
1456
1457
1458
1459
1460
1461
1462
1463
1464
1465
1466
1467
1468
1469
1470
1471
1472
1473
1474
1475
1476
1477
1478
1479
1480
1481
1482
1483
1484
1485
1486
1487
1488
1489
1490
1491
1492
1493
1494
1495
1496
1497
1498
1499
1500
1501
1502
1503
1504
1505
1506
1507
1508
1509
1510
1511
1512
1513
1514
1515
1516
1517
1518
1519
1520
1521
1522
1523
1524
1525
1526
1527
1528
1529
1530
1531
1532
1533
1534
1535
1536
1537
1538
1539
1540
1541
1542
1543
1544
1545
1546
1547
1548
1549
1550
1551
1552
1553
1554
1555
1556
1557
1558
1559
1560
1561
1562
1563
1564
1565
1566
1567
1568
1569
1570
1571
1572
1573
1574
1575
1576
1577
1578
1579
1580
1581
1582
1583
1584
1585
1586
1587
1588
1589
1590
1591
1592
1593
1594
1595
1596
1597
1598
1599
1600
1601
1602
1603
1604
1605
1606
1607
1608
1609
1610
1611
1612
1613
1614
1615
1616
1617
1618
1619
1620
1621
1622
1623
1624
1625
1626
1627
1628
1629
1630
1631
1632
1633
1634
1635
1636
1637
1638
1639
1640
1641
1642
1643
1644
1645
1646
1647
1648
1649
1650
1651
1652
1653
1654
1655
1656
1657
1658
1659
1660
1661
1662
1663
1664
1665
1666
1667
1668
1669
1670
1671
1672
1673
1674
1675
1676
1677
1678
1679
1680
1681
1682
1683
1684
1685
1686
1687
1688
1689
1690
1691
1692
1693
1694
1695
1696
1697
1698
1699
1700
1701
1702
1703
1704
1705
1706
1707
1708
1709
1710
1711
1712
1713
1714
1715
1716
1717
1718
1719
1720
1721
1722
1723
1724
1725
1726
1727
1728
1729
1730
1731
1732
1733
1734
1735
1736
1737
1738
1739
1740
1741
1742
1743
1744
1745
1746
1747
1748
1749
1750
1751
1752
1753
1754
1755
1756
1757
1758
1759
1760
1761
1762
1763
1764
1765
1766
1767
1768
1769
1770
1771
1772
1773
1774
1775
1776
1777
1778
1779
1780
1781
1782
1783
1784
1785
1786
1787
1788
1789
1790
1791
1792
1793
1794
1795
1796
1797
1798
1799
1800
1801
1802
1803
1804
1805
1806
1807
1808
1809
1810
1811
1812
1813
1814
1815
1816
1817
1818
1819
1820
1821
1822
1823
1824
1825
1826
1827
1828
1829
1830
1831
1832
1833
1834
1835
1836
1837
1838
1839
1840
1841
1842
1843
1844
1845
1846
1847
1848
1849
1850
1851
1852
1853
1854
1855
1856
1857
1858
1859
1860
1861
1862
1863
1864
1865
1866
1867
1868
1869
1870
1871
1872
1873
1874
1875
1876
1877
1878
1879
1880
1881
1882
1883
1884
1885
1886
1887
1888
1889
1890
1891
1892
1893
1894
1895
1896
1897
1898
1899
1900
1901
1902
1903
1904
1905
1906
1907
1908
1909
1910
1911
1912
1913
1914
1915
1916
1917
1918
1919
1920
1921
1922
1923
1924
1925
1926
1927
1928
1929
1930
1931
1932
1933
1934
1935
1936
1937
1938
1939
1940
1941
1942
1943
1944
1945
1946
1947
1948
1949
1950
1951
1952
1953
1954
1955
1956
1957
1958
1959
1960
1961
1962
1963
1964
1965
1966
1967
1968
1969
1970
1971
1972
1973
1974
1975
1976
1977
1978
1979
1980
1981
1982
1983
1984
1985
1986
1987
1988
1989
1990
1991
1992
1993
1994
1995
1996
1997
1998
1999
2000
2001
2002
2003
2004
2005
2006
2007
2008
2009
2010
2011
2012
2013
2014
2015
2016
2017
2018
2019
2020
2021
2022
2023
2024
2025
2026
2027
2028
2029
2030
2031
2032
2033
2034
2035
2036
2037
2038
2039
2040
2041
2042
2043
2044
2045
2046
2047
2048
2049
2050
2051
2052
2053
2054
2055
2056
2057
2058
2059
2060
2061
2062
2063
2064
2065
2066
2067
2068
2069
2070
2071
2072
2073
2074
2075
2076
2077
2078
2079
2080
2081
2082
2083
2084
2085
2086
2087
2088
2089
2090
2091
2092
2093
2094
2095
2096
2097
2098
2099
2100
2101
2102
2103
2104
2105
2106
2107
2108
2109
2110
2111
2112
2113
2114
2115
2116
2117
2118
2119
2120
2121
2122
2123
2124
2125
2126
2127
2128
2129
2130
2131
2132
2133
2134
2135
2136
2137
2138
2139
2140
2141
2142
2143
2144
2145
2146
2147
2148
2149
2150
2151
2152
2153
2154
2155
2156
2157
2158
2159
2160
2161
2162
2163
2164
2165
2166
2167
2168
2169
2170
2171
2172
2173
2174
2175
2176
2177
2178
2179
2180
2181
2182
2183
2184
2185
2186
2187
2188
2189
2190
2191
2192
2193
2194
2195
2196
2197
2198
2

50 adsorption processes. The observed decrease of ΔG^0 (ranging from -18 to -21 kJ/mol) implies
51 a physical nature of the adsorption. The post-adsorption L and RD residues were subjected to
52 solid state cultivation using the fungus *Ganoderma resinaceum* GA1M yielding mycelium-
53 based biocomposites. The investigations revealed that the biocomposites were free from Acid
54 orange 7. The approaches presented here demonstrate that L and RD industrial by-products
55 can be successfully applied for the adsorption of Acid orange 7 while producing harmless
56 mycelium-based biocomposites through solid state fermentation using *G. resinaceum* GA1M.

57
58 Keywords: azo dye; acid orange 7 adsorption; lavender and rose by-products; isotherm
59 models; *Ganoderma resinaceum*; mycelium-based biocomposites

60 61 1. Introduction

62 2.

63 Azo dyes are among the most widely used by industry colorants. More than 60% of the
64 synthetic organic dyes generated are azo dyes [1]. These dyes are extensively used in the
65 textile, leather, plastic, and food industries due to their vivid and intense colors. More than
66 2000 azo dyes have been synthesized and it is not surprising that due to their important
67 industrial role their toxicity was widely studied. In general, azo dyes possess photolytic
68 stability and only negligibly biodegrade in nature. This stability poses an environmental risk.
69 Moreover, some of the azo dyes are known to be toxic and carcinogenic. Specifically, the
70 metabolization and decomposition of azo dyes lead to the production of aromatic amines of
71 which some are known as human carcinogens (Group III A 1 of the German MAK III list)
72 and compounds posing risks to animals thereby also posing risks to human health (Group III
73 A 2) [2]. In the European Union (EU) some azo dyes are restricted by several regulations,
74 such as: REACH, Toy safety directive, and the EU food contact material framework.

75 Therefore, precautions must be taken to eliminate azo dyes from waste waters and to avoid
76 human exposure to the most dangerous ones.

77 The problem is also related to the worldwide growing demand for water with high enough
78 quality, necessity to protect water resources and to purify the wastewaters [3]. The overall
79 increase of the industrial production capacity (textile, mining, papers, plastics, etc.) lead to
80 extensive usage of water and obtaining of large volumes wastewaters. Dying and textile
81 industry are among the largest consumers of water and around 15% of the dyes are released
82 in the environment without proper treatment [4]. These practices pose serious environmental
83 risks and hence proper purification methods and technologies should be investigated and
84 introduced.

85 Acid orange 7 is an azo dye with an appealing red-orange color. It is mainly used for silk and
86 wool dyeing, polyamide fiber fabric of direct printing, leather and paper coloration, hair
87 dyeing products, and is also utilized as an indicator and biological stain [5]. This azo dye is
88 produced by coupling of *p*-aminobenzenesulfonic acid (after diazotation) and 2-naphtol.

89 Reductive cleavage by bacteria or degradation by chemical or physical factors could result in
90 the production of corresponding aromatic amino compounds. Brüscheiler and Merlot [6]
91 reported that the *o*- and *p*-aminobenzenesulfonic acid could be mutagenic and are found in
92 some wool, cotton and other cellulose fibers. *P*-aminobenzenesulfonic acid was amongst the
93 most frequently determined aromatic amines, found in 37 textile samples in concentrations in
94 the 100–442 mg/kg range [5].

95 Various methods for decontamination and removal of compounds like azo dyes were
96 proposed and investigated. Some of these methods are based on physicochemical interactions
97 (such as flocculation, adsorption, ozonation, electrolytic and photooxidation, etc.),
98 phytoremediation [7] and others rely on microbial or fungal degradation [8-12]. Taheri et al.
99 [13] performed a study for the removal of two azo dyes: Acid orange 7 and Acid red 18 by

100 several methods to compare the costs and effectiveness of the methods for decontamination.
1
2 101 The authors found that the utilization of activated carbon in combination with membrane
3
4
5 102 filtration in a sequencing batch reactor showed the most promising results. However, the
6
7 103 initial investments are usually higher than performing a simple adsorption or microbial/fungal
8
9 104 degradation. Numerous adsorbents have been tested for the removal of azo dyes [13-16] with
10
11
12 105 the most significant advantage being the utilization of renewable and cheap resources as
13
14 106 adsorbents. Such abundant and easily available materials are very often by-products / wastes
15
16 107 from the food and agricultural industries which generate large amounts of biodegradable
17
18 108 phytomass annually.
19
20
21 109 The essential oil industry, because of the usually low amount of the essential oil in the raw
22
23 110 plant material, produces tonnes of solid by-products which are commonly discarded [17].
24
25
26 111 Lavender and roses are amongst the most processed crops in the essential oil industry and the
27
28 112 by-products obtained from their distillation could be used as a cheap, abundant, and
29
30 113 biodegradable adsorbent for pollutant removal. The solid lavender and rose post-distillation
31
32 114 biomass have been successfully employed in numerous works for the removal of heavy
33
34 115 metals in model studies and in waste waters [17] but few studies have specifically focused on
35
36 116 the application for the adsorption of organic pollutants [18, 19]. Additionally, the residues
37
38 117 from the adsorption of azo dyes could be subjected to further degradation by higher fungi,
39
40 118 which are known for their abilities to produce enzymatic complexes able to degrade
41
42 119 lignocellulosic materials and polyphenols [20-25].
43
44
45
46 120 Hence the aim of the present work was to investigate the applicability of rose and lavender
47
48 121 industrial post-distillation by-products as natural adsorbents for removal of the azo dye Acid
49
50 122 orange 7 and to study the factors, kinetics, thermodynamic parameters, and further fungal
51
52 123 biodegradation of the post-adsorption residues. The study proposes an innovative method for
53
54 124 lavender and rose post-distillation by-products valorization. It is known that due to their high
55
56
57
58
59
60
61
62
63
64
65

125 polyphenolic compounds content their direct disposal in landfills are likely environmentally
126 harmful and therefore the method would contribute to sustainability, a circular economy, and
127 zero waste approaches in general.

128

129 2. Materials and methods

130

131 2.1. Samples and reagents

132 Lavender (bio-certified *Lavandula angustifolia* Mill., “Sevtopolis” cultivar) – L and rose
133 (bio-certified *Rosa Damascena* Mill.) – RD, by-products from industrial steam distillation of
134 fresh plant stems and flowers were provided by the ECOMAAT distillery (Mirkovo, region
135 of Sofia, Bulgaria; 2021 harvest). The L and RD by-products were collected when the
136 distillation was finished: for RD residues the mass was pumped out from the still and after
137 passing through a screw conveyor the solid residue was separated from the liquid phase; for L
138 residue the mass was removed from the baskets in the still and collected. The solid residues
139 were inspected for impurities and dried. The dried rose and lavender were washed with
140 distilled water (100 g with 1600 mL water; added in portions of 400 mL) on a Buchner
141 funnel. The residual mass was dried, milled, and sieved. For adsorption of the azo dye, the
142 biomass fraction with particle size 100-250 μm were used.

143 Acid orange 7 (4-(2-Hydroxy-1-naphthylazo) benzenesulfonic acid sodium salt) was obtained
144 from local distributors (Table 1).

145

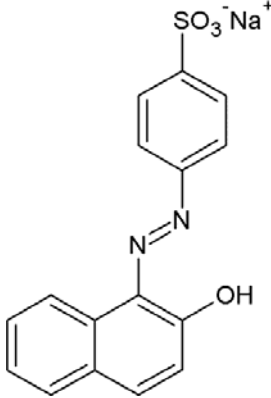
146

147

148

149

150 Table 1. Characteristics of the azo dye Acid orange 7

Name	Structure	Molecular formula	Mw (g/mol)	Density, g/mL	Solubility, g/L (20°C)
Acid orange 7		C ₁₆ H ₁₁ N ₂ NaO ₄ S	350.3	1.6	27

151

152 2.2. Methods

153

154 2.2.1. Adsorption procedure

155 The adsorption of the azo dye was carried out as follow: 20 mL water solution of Acid orange
 156 7 with specified concentrations (20, 40, 60, 80 and 100 mg/L) were added to 1 g adsorbent in
 157 a 50 mL centrifuge tube and the tubes were placed on a laboratory shaker MLW THYS 2
 158 (VEB MLW Labortechnik Ilmenau, Germany), placed in a thermally controlled laboratory
 159 oven (the experiments were performed at three temperatures: 293 K, 303 K and 313 K). The
 160 shaker was started (100 rpm) and at a specified time (2.5, 5, 10, 20, 40, 60, 90 and 120
 161 minutes) a centrifuge tube was removed from the shaker and the mass was filtered first
 162 through a paper filter and second through a syringe filter CA 0.45 μm (Isolab, Germany).
 163 Adsorption of the filtrate was measured at 500 nm using LLG-uniSPEC 2 UV-Vis
 164 spectrophotometer (LLG Labware, Germany). The concentration of non-adsorbed Acid
 165 orange 7 was calculated using a calibration curve, prepared with water solutions of the dye
 166 with known concentrations. The adsorption of Acid orange 7 by L and RD residues at

167 different pH mediums was performed as described above using 100 mg/L solution of the dye
168 at 313 K in – for pH 1.05: 0.05 M sulfuric acid; for pH 3.50: 0.05 M citrate buffer; for pH
169 5.50: 0.05 M citrate buffer; for pH 10.75: 0.05 M carbonate buffer.

170 2.2.2. Solid-state cultivation of *Ganoderma resinaceum* using L and RD residues from dye
171 adsorption as substrates for mycelium-based biocomposite preparation.

172 1) Substrate Preparation Procedure: The dried residue from dye adsorption (150 g) was
173 humidified with a solution with the following composition (g/L): Yeast extract: 2.0; Peptone:
174 2.0; KH₂PO₄: 0.5; K₂HPO₄: 1.0; MgSO₄: 0.5 up to final 65-70% moisture. 0.1% of calcium
175 carbonate was added, mixed well and the mixture was transferred into growing bags (SacO₂,
176 Belgium). The mixture was sterilized at 394 K for 45 min, cooled down and used as a feeding
177 substrate for the next procedure of inoculation and cultivation.

178 2) Fungi *Ganoderma resinaceum* GA1M

179 The macrofungal strain *Ganoderma resinaceum* GA1M is part of the microbial collection of
180 the Department of Biotechnology, University of Food Technologies, Plovdiv, Bulgaria and is
181 maintained at 4°C on Mushroom Complete medium (MCM) containing 20.0 g/L of glucose,
182 0.5 g/L of KH₂PO₄, 1.0 g/L of K₂HPO₄, 0.5 g/L of MgSO₄, 2.0 g/L of peptone, 2.0 g/L of
183 yeast extract, 2.0 g/L of agar, pH 4.8–5.2, and was subcultured every 30 days onto fresh
184 medium. The strain was previously isolated and molecularly identified [200].

185 3) Inoculation of the substrate and mycelium growth:

186 The inoculation of the substrate was performed with vegetative inoculum obtained through
187 cultivation of *G. resinaceum* in MCM broth at 301 K and 220 rpm for 7 days until pellets
188 were formed. Sterile filtration was used for the collection of the pellets which were then used
189 for the inoculation of the mixture. The determination of the pellets dry weight was performed
190 on a moisture analyzer (RADWAG, Poland).

191 The mixing of the pellets (10 % w/w) with the substrate was made in sterile conditions in the
192 growing bag, which were placed at 298 K in darkness. The substrate was fully enveloped by
193 the mycelium for 7 days. Each growing bag was observed and mixed daily to ensure the full
194 coverage of the substrates particles and uniform mycelium growth. To obtain mycelium-
195 based biocomposites with proper sample geometry, aseptic transfer of the substrate/mycelium
196 mixture into molds and further cultivation according to [20] was performed.

197 4) Determination of residual Acid orange 7 in the biocomposites.

198 50 g of the mycelium-based biocomposites prepared by the fungal growth on L and RD post-
199 adsorption residues was milled and extracted with 500 mL deionized water at 333 K and
200 constant stirring (100 rpm) for 1 hour. The mass was filtered and the solid residue was
201 subjected to the same extraction procedure 2 more times. The combined filtrates were
202 evaporated to 100 mL final volume and lyophilized. The lyophilized extract was dissolved in
203 deionized water at 100 mg/mL concentration and filtered through a syringe filter CA 0.45 μm
204 (Isolab, Germany). Absorption of the filtrate was measured at 500 nm using LLG-uniSPEC 2
205 UV-Vis spectrophotometer (LLG Labware, Germany) and the concentration of the Acid
206 orange 7 was calculated using a calibration curve, prepared with water solutions of the azo
207 dye with known concentrations.

208

209 2.2.3. Infrared spectroscopy

210 Infrared spectra of the rose and lavender biomass (before and after adsorption of Acid orange
211 7) were taken in KBr (4 mg sample) using Bruker VERTEX 70 FT-IR Spectrometer (USA)
212 with 25 scans of the samples.

213

214 2.2.4. Sample morphology determination by Scanning electron microscopy (SEM)

1
2
3
4
5
6
7
8
9
10
11
12
13
14
15
16
17
18
19
20
21
22
23
24
25
26
27
28
29
30
31
32
33
34
35
36
37
38
39
40
41
42
43
44
45
46
47
48
49
50
51
52
53
54
55
56
57
58
59
60
61
62
63
64
65

215 The morphology analyses of the samples were performed by digitized Scanning Electron
216 Microscope Philips 515 (The Netherlands). Before the analyses, micro-quantities of the
217 samples have been fixed on standard microscope pins using adhesive tape and then covered
218 by Au-Pd metal film for better conductivity. An accelerating voltage of 7 kV was applied on
219 the electrons in this experiment.

220

221 2.2.5. Isotherm modelling

222 The amount of dye adsorbed per unit mass of adsorbent (q_e , mg/g) was calculated using the
223 mass balance Eq. 1:

224

$$225 \quad q_e = \frac{c_0 - c_e}{m} V \quad \text{Eq. 1}$$

226

227 where V is the solution volume, L; c_0 and c_e are initial and equilibrium concentration, mg/L;
228 m is the adsorbent mass, g.

229 The most widely used models for description and explanation of adsorption isotherms are

230 Langmuir, Freundlich and Temkin models.

231

232 1) Langmuir isotherm model

233 Langmuir derived an empirical model that postulates a monolayer adsorption of molecules

234 onto a morphologically homogeneous adsorbent surface containing at a fixed number of

235 active adsorption sites, with no lateral interactions. Langmuir made several assumptions, the

236 most important is one-site occupancy adsorption, which occurs at specific homogeneous sites

237 on the surface of the adsorbent and proposes an empirical nonlinear model [26]. Langmuir

238 hypothesized that all the adsorption sites are identical in affinity and energy. The model

239 further assumes that the intermolecular attractive forces diminish steadily with distance

240 increases. The original non-linear form of the Langmuir equation is expressed as:

241

$$q_e = \frac{q_m K_L c_e}{1 + K_L c_e} \quad \text{Eq. 2}$$

243

244 where q_m is the maximum adsorption capacity, mg/g; K_L is Langmuir constant associated

245 with the affinity of the binding sites and energy of adsorption, L/g.

246 The linear form of Langmuir Eq. 2 is expressed as [27]:

247

$$\frac{c_e}{q_e} = \frac{c_e}{q_m} + \frac{1}{q_m K_L} \quad \text{Eq. 3}$$

249

250 2) Freundlich isotherm model

251 The Freundlich model postulates a multilayer adsorption process, with non-uniform

252 distribution of adsorption enthalpy and affinities onto the heterogeneous adsorbent surface

253 without lateral interaction. The energetically favored binding sites are theorized to be

254 occupied first and the binding strength decreases sequentially with increased coverage of the

255 binding sites. The non-linear Freundlich equation is expressed as [28]:

256

$$q_e = K_F c_e^{1/n} \quad \text{Eq. 4}$$

258

259 where K_F is Freundlich constant associated with adsorption capacity, L/g; n is an empirical

260 constant connected to adsorption intensity.

261 The linear form of Eq. 4 is expressed as [27]:

262

263 $\ln q_e = \ln K_F + \frac{1}{n} \ln c_e$ Eq. 5

264

265 3) Temkin isotherm model

266 The Temkin isotherm model considers the effect of indirect adsorbate-adsorbing species

267 interactions on adsorption. It postulates that the heat of adsorption as a function of

268 temperature of all the molecules in the layer reduces linearly rather than logarithmically with

269 surface coverage due to adsorbent-adsorbate interactions [29]. The non-linear Temkin

270 isotherm equation is given by:

271

272 $q_e = \frac{RT}{b} \ln(A_T c_e) = B \ln(A_T c_e)$ Eq. 6

273

274 where T is the absolute temperature, K; $R = 8.314$ is the universal gas constant, J/(mol.K); A_T

275 is the equilibrium binding constant, L/g; b is the variation in adsorption energy, J/mol; B is

276 the Temkin constant.

277 The linear form of Temkin equation is expressed as [27]:

278

279 $q_e = B \ln A_T + B \ln c_e$ Eq. 7

280

281 4) Thermodynamic parameters determination

282 Thermodynamic parameters were determined using the thermodynamic equilibrium

283 distribution constants k_d at the studied temperatures:

284

284 $k_d = \frac{q_e}{c_e}$ Eq. 8

285

285 The coefficients k_d were calculated by the method suggested by Khan and Singh [30] from

286 the intercept of the plots of $\ln(q_e/c_e)$ vs. q_e . The coefficient k_d has the dimension L/g. It needs

287 to be converted into dimensionless form K_e by multiplying with the density of water (1000
288 g/L) to be used in the thermodynamic equation [31]:

$$289 \quad K_e = 1000k_d \quad \text{Eq. 9}$$

290 Then, the change in Gibbs free energy ΔG^0 , J/mol, enthalpy ΔH^0 , J/mol, and entropy ΔS^0 ,
291 were calculated from the Van't-Hoff equation:

$$292 \quad \ln K_e = \left(\frac{-\Delta H^0}{R} \right) \frac{1}{T} + \frac{\Delta S^0}{R} \quad \text{Eq. 10}$$

293 From the plot of $\ln K_e$ as a function of $1/T$ (van't Hoff plot) according to Eq. 10 the values of
294 ΔH^0 and ΔS^0 J/(mol.K), were calculated using the slope and intercept of the straight lines
295 respectively.

296 The values of ΔG^0 were calculated using Eq. 11.

$$297 \quad \Delta G^0 = \Delta H^0 - T\Delta S^0 \quad \text{Eq. 11}$$

299 2.3. Statistical analysis

300 The experiments were performed in triplicate and data values are expressed as mean \pm SD
301 (standard deviation). Statistical analysis was carried out by one way ANOVA (Tukey's *post*
302 *hoc* test; $p < 0.05$).

304 3. Results and discussion

306 3.1. Kinetics of the adsorption of Acid orange 7 on L and RD by-products

307 One of the most important parameters influencing the adsorption process is the contact time
308 of the solution with the adsorbent. Fig. 1 shows the kinetics of the adsorption and the

1
2
3
4
5
6
7
8
9
10
11
12
13
14
15
16
17
18
19
20
21
22
23
24
25
26
27
28
29
30
31
32
33
34
35
36
37
38
39
40
41
42
43
44
45
46
47
48
49
50
51
52
53
54
55
56
57
58
59
60
61
62
63
64
65

309 dependence of the Acid orange 7 adsorption process on the contact time, temperature and
310 initial dye concentration. In the beginning the adsorption was very rapid and at the second
311 minute most of the dye was already adsorbed to the adsorbent surface. The equilibrium for
312 the adsorption of the Acid orange 7 was determined at 60 min for RD (293 K) and for L (at
313 the three investigated temperatures). For RD (at 303 K and 313 K) a constant but negligible
314 rise of the adsorbed dye was observed until the 120 min. The higher temperatures slightly
315 increased the adsorption of the azo dye on the L and RD. Increase of the initial concentration
316 from 20 to 100 mg/L azo dye lead to an increase of the adsorbed amount from 0.32 to 1.63
317 mg/g adsorbent L at 293 K, from 0.28 to 1.61 mg/g adsorbent L at 303 K and from 0.28 to
318 1.58 mg/g adsorbent L at 313 K. The RD residue as adsorbent demonstrated slightly higher
319 capacity: with the increase of the initial concentration of the Acid orange 7 from 20 to 100
320 mg/L the adsorbed amount incremented from 0.35 to 1.74 mg/g RD adsorbent at 293 K, from
321 0.34 to 1.73 mg/g RD adsorbent at 303 K and from 0.34 to 1.71 mg/g RD adsorbent at 313 K.
322 The highest adsorption capacity was demonstrated by both adsorbents with the highest initial
323 concentration of 100 mg/L azo dye. These results correlate well with previously reported
324 literature data for adsorption of Metanil yellow azo dye on bottom ash and de-oiled soya [15],
325 adsorption of Basic blue 41 on *Juniperus excelsa* residues [32], and combined adsorption and
326 decolorization of Remazol brilliant violet 5R and Sunset Yellow [23].

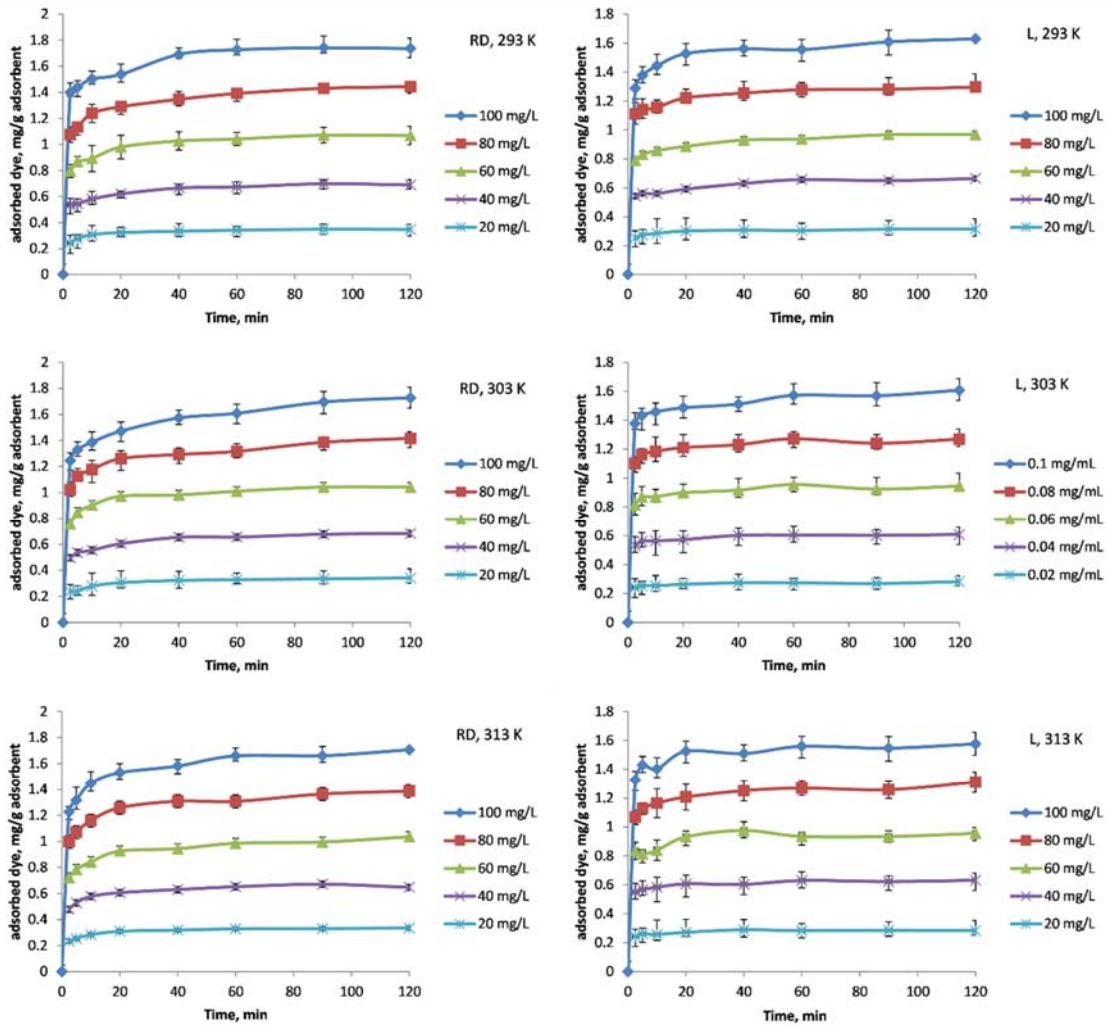


Fig. 1 Effect of the contact time (0-120 min), temperature (293, 303 and 313 K) and initial concentration of Acid orange 7 (20, 40, 60, 80 and 100 mg/L) on the dye removal using L and RD by-products. Amount of RD and L adsorbents: 1 g; volume of dye solution: 20 mL; pH=7.05; shaking speed 100rpm

Based on the data from kinetic of adsorption of the Acid orange 7 on L and RD adsorbents were determined the equilibrium concentrations c_e , mg/L (Table 2) for the three investigated temperatures.

15
16
17
18
19
20
21
22 337
23
24 338
25
26
27 339
28
29
30
31
32
33
34
35
36
37
38
39
40
41
42
43
44
45
46
47
48
49 340
50
51
52
53
54
55
56
57
58
59
60
61
62
63
64
65

Table 2. Equilibrium concentration (c_e , mg/L) at 20, 40, 60, 80 and 100 mg/L initial concentrations (c_0 , mg/L) and temperatures 293, 303 and 313 K for L and RD. Amount of RD and L adsorbents: 1 g; volume of dye solution: 20 mL; pH=7.05; shaking speed 100rpm

c_0 , mg/L	c_e , mg/L					
	L			RD		
	293K	303K	313K	293K	303K	313K
20	5.85±0.15 ^a	5.37±0.44 ^{a,b}	4.19±0.42 ^b	3.27±0.20 ^c	2.92±0.12 ^{c,d}	2.51±0.29 ^d
40	8.45±0.08 ^b	9.61±0.49 ^a	6.74±0.32 ^d	7.66±0.37 ^c	5.87±0.24 ^c	5.06±0.29 ^f
60	12.21±0.21 ^{a,b}	12.76±0.62 ^a	11.60±0.51 ^b	8.21±0.20 ^c	7.90±0.19 ^c	6.42±0.20 ^d
80	14.47±0.14 ^b	16.55±0.29 ^a	15.18±0.26 ^a	10.68±0.27 ^c	9.19±0.35 ^d	8.45±0.22 ^d
100	21.17±0.24 ^a	19.65±0.45 ^b	18.54±0.24 ^c	14.68±0.18 ^d	13.60±0.21 ^c	12.98±0.79 ^f

^{a,b,c,d,e,f} Different letters in a row mean statistically different values ($p < 0.05$)

1 341 The influence of the pH medium was investigated at five different pH values (Table 3). At
2
3 342 lower pH (below 5.5) the effectiveness of adsorption increased and for L adsorbent at pH 1.5
4
5 343 the removal of the dye reached almost 99%. The RD was also effective at pH 3.5 and 5.5
6
7 344 (98.75% removal). In general it could be concluded that the acidic medium increased the
8
9
10 345 effectiveness of dye removal. The Acid orange 7 is an anionic dye and in acidic medium the
11
12 346 sulfo-groups will be protonated. In the same time at lower pH the net charge of the adsorbent
13
14 347 will be lower due to protonation of the carboxyl groups considered among the main
15
16
17 348 functional groups favoring adsorption [33] having in mind that the amount of pectic
18
19 349 substances in the RD and L are around 10-15% [17, 34]. By this way the electrostatic
20
21
22 350 repulsion will be lower and will favor the adsorption. The results for adsorption at higher pH
23
24 351 (only 2.50–3.75% removal) suggested that the electrostatic interactions plays important role
25
26
27 352 in the sorption process. These results are in accordance with the findings of Wu et al. [35]
28
29 353 and Pelosi et al. 2013 [36] investigating the Acid orange 7 adsorption on waste brewery's
30
31 354 yeast and *Salvinia natans* biomass, respectively. However, Wu and coworkers [35] found that
32
33
34 355 above pH 5 the efficiency of waste brewery's yeast as adsorbent lowered significantly while
35
36 356 the effectiveness of L and RD at neutral pH was still 87.03% and 92.15%, respectively. These
37
38
39 357 findings are important because operating on a large scale at neutral medium than in acidic
40
41 358 condition is easier and beneficial for the environment. Besides, further neutralization of both
42
43
44 359 the spent adsorbent and the solution will be necessary. Except electrostatic repulsion between
45
46 360 negatively charged sulfo and carboxyl groups other interactions (chemical or physical), such
47
48
49 361 as: hydrogen bonding, coordinative bonding, hydrophobic interactions, double bond
50
51 362 attraction, pore filling, partitioning, could be involved in the mechanism of sorbent retention
52
53 363 [3].
54
55

56 364

57
58
59
60
61
62
63
64
65

365 Table 3. Influence of the pH medium on the adsorption of Acid orange 7 on L and RD.
 366 Adsorbed amount: mg/g (in brackets is given the efficiency of the adsorption in percentage).
 367 Adsorbent: 1g; initial azo dye: 20 mL 100 mg/L (2 mg dye in the volume); temperature 313
 368 K; shaking speed 100rpm

pH	1.05	3.50	5.50	7.05	10.75
L	1.975±0.08 (98.75)	1.95±0.09 (97.50)	1.775±0.1 (88.75)	1.63±0.08 (81.50)	0.075±0.02 (3.75)
RD	1.80±0.07 (90.06)	1.975±0.08 (98.75)	1.975±0.08 (98.75)	1.74±0.08 (87.00)	0.05±0.02 (2.50)

369
 370 Table 4 presents the results for adsorption of Acid orange 7 by L and RD compared with
 371 different adsorbents found in the literature. Although, the L and RD residues showed lower
 372 adsorption capacities compared with other adsorbents, it should be noted that the results were
 373 achieved at neutral pH values. At acidic pH medium the effectiveness of the azo dye removal
 374 reached 98.75% for both adsorbents.

375
 376 Table 4. Comparison of adsorption capacities of different adsorbents of Acid orange 7

Adsorbent	Conditions	Adsorption capacity	
		(mg/g) / removal efficiency, %	References
<i>Salvinia natans</i> biomass	293 K, pH 1	46.53 / 46.53%	[36]
Canola waste	288 K	24.23/ >99%	[37]

1	Polypyrrole/nanosilica	328 K, pH 3	24.93	[38]
2	composite			
3				
4		293 K, pH 2.5,	8.96/	
5	Canola stalks	100 mg/L dye	>90%	[33]
6				
7			3.78/	
8	Bottom ash		68%	
9		303 K, pH 2		[39]
10			7.61/	
11	De-oiled soya		58%	
12				
13	Beech wood sawdust	303 K	5.06	[40]
14				
15	Waste brewery's yeast	303 K, pH 2	3.561	[35]
16				
17	Lavender by-product	293 K, pH	1.63 /	
18				present study
19	(L)	7.05, 1 g	81.50%	
20		adsorbent, 20		
21				
22	<i>Rosa Damascena</i> by-	mL 100	1.74 /	
23				present study
24	product (RD)	mg/mL (2 mg	87.00%	
25		dye total)		
26				

377

378

379 3.2. Infrared spectroscopy and morphology of L and RD by-products and post-adsorption L

380 and RD residues

381

382 Infrared spectroscopy is a powerful tool that can provide meaningful information about the

383 functional groups of investigated substances. Fig. 2a presents the infrared spectra of the Acid

384 orange 7. A broad and characteristic peak corresponding to the O-H stretching vibrations was

385 observed at 3448 cm^{-1} . The bands at 1048 and 1387 cm^{-1} could be attributed to the azo (–

386 N=N-) bond stretching movements, while the ones at 1035, 1122 and 1186 cm^{-1} are
387 characteristic peaks indicating the presence of sulfo groups [41]. Additionally, a band due to
388 aromatic ring stretching was observed at 1511 cm^{-1} . The RD and L by-products (Fig. 2b and
389 2c) exhibited characteristic bands at 3421 and 3427 cm^{-1} due to presence of OH groups (main
390 functional group in the polysaccharides). Peaks at 1636-1647 and 1734-1735 cm^{-1} could be
391 assigned to stretching and vibrations of the carboxyl groups from the pectic moieties. The
392 infrared spectra of post-adsorption RD and L residues are presented in Fig. 2c and 2e,
393 respectively. The most significant differences could be observed around 1500-1560 cm^{-1}
394 where a new peak at 1540 cm^{-1} (for RD post-adsorption residue) and 1541 cm^{-1} (for L post-
395 adsorption residue) could be found. These bands are a result of the aromatic ring stretching
396 vibrations from the aromatic moieties of Acid orange 7 suggesting successful adsorption of
397 the dye onto the surface of the RD and L by-products.

398

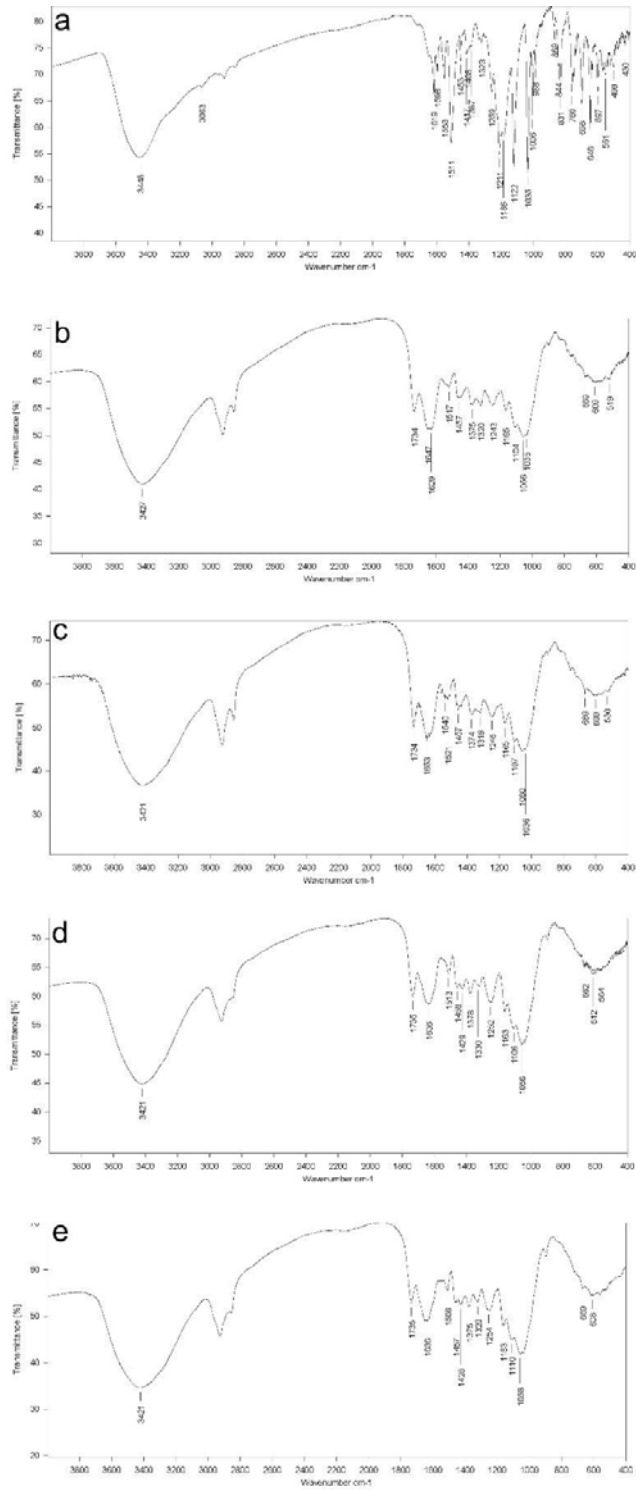
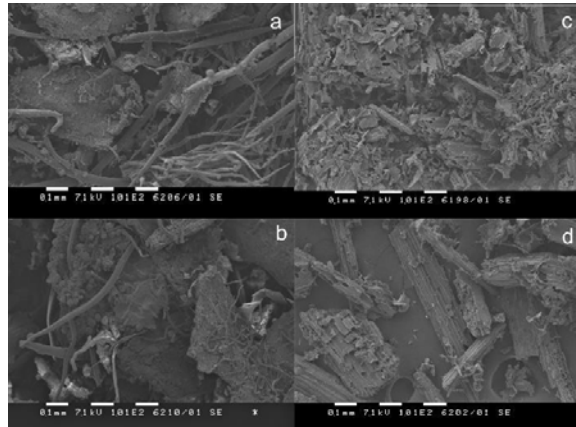


Fig. 2 Infrared spectra of Acid orange 7 (a); rose by-products: before (b) and after adsorption (c); lavender by-products: before (d) and after adsorption (e)

403 Furthermore, the morphology of the adsorbents and the post-adsorption residues of RD and L
404 were investigated by SEM and the observed image is presented in Fig. 3. The RD by-product
405 image revealed the presence of a fiber-type structure probably due to polysaccharide chains
406 while the L by-product could be characterized with a fluffier and more porous surface. The
407 post-adsorption residues generally retain their structure. Although, some studies [16, 42]
408 suggested that there is a significant difference in the adsorbent structure before and after
409 adsorption, in our case no observable changes in the RD and L post-adsorption residues
410 morphology, compared to the RD and L by-products, could be observed. This could be
411 explained with the physical type of the adsorption process of the Acid orange 7 onto the
412 surface of the RD and L by-products.

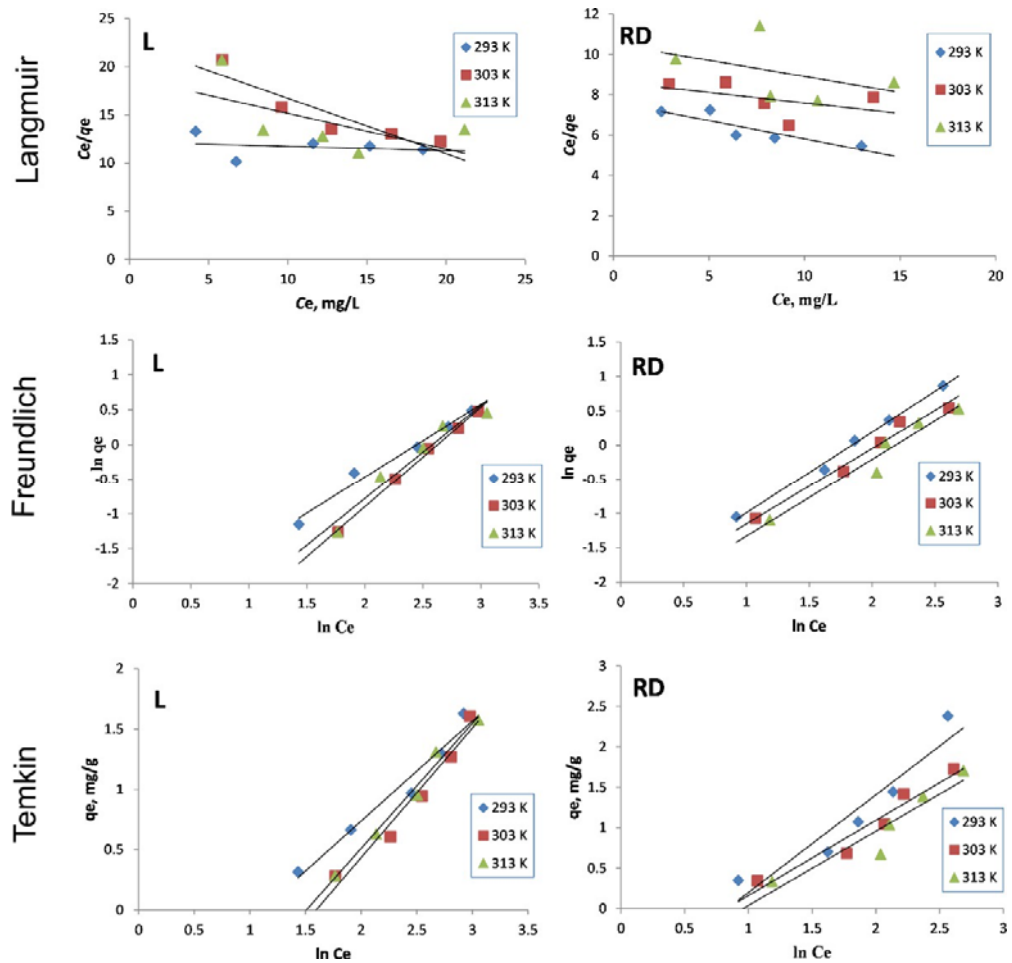


414
415 **Fig. 3** Morphological analysis by SEM of the RD (a. before adsorption; b. after adsorption)
416 and L (c. before adsorption; d. after adsorption) residues

418 3.3. Adsorption isotherms parameters determination

419
420 The adsorption isotherm characterizes the equilibrium state of molecules distribution between
421 the liquid and solid phase [43]. To evaluate the applicability of different isotherm models
422 (Langmuir, Freundlich, Temkin) to describe the process of adsorption their linearized form

423 was used (Eq. 3, 5 and 7, section 2.2.5). The Langmuir isotherm model assumes that
 424 adsorption occurs on a relatively homogenous surface with limited interactions in the surface
 425 plane. The Freundlich model empirically describes adsorption on non-homogenous, porous
 426 surfaces. The Temkin isotherm model describes interactions of heterogeneous solid surfaces
 427 with molecules from a solution and this assumption is made on the basis that temperature
 428 increases lead to decreases of surface covering. The correlation of the models to the
 429 experimental results is expressed by fitted plots and presented in Fig. 4.



431
 432 **Fig. 4** Langmuir, Freundlich and Temkin isotherms of Acid orange 7 adsorption on L and RD
 433 residues for 293, 303 and 313 K

434

1
2 435 The parameters of the Langmuir, Freundlich and Temkin isotherm equations were calculated
3
4
5 436 and are presented in Table 5. The coefficients of determination showed that the Freundlich
6
7 437 equation better described the adsorption of Acid orange 7 using RD and L post-distillation
8
9
10 438 by-products than the Langmuir and Temkin models. Similar results were obtained by Khosla
11
12 439 et al. [44] investigating adsorption of Acid orange 7 on aluminum oxide nanoparticles. This
13
14 440 suggests a multilayer adsorption process and confirms the heterogeneous structure of the
15
16
17 441 surface of both adsorbents without lateral interactions. The coefficient n in the Freundlich
18
19 442 equation connected to adsorption intensity is practically not influenced by the temperature
20
21
22 443 and the type of the adsorbent. The values of the coefficient K_F showed higher adsorption
23
24 444 capacity for RD compared with L's capacity, at the three temperatures studied. In opposite of
25
26
27 445 the established from Khosla et al. [44], the values of the coefficient decreased with the
28
29 446 temperature rise, which probably means a decrease in the binding forces at higher
30
31
32 447 temperatures.

15
 16
 17
 18
 19
 20
 21
 22 448
 23
 24 449
 25
 26
 27
 28
 29
 30
 31
 32
 33
 34
 35
 36
 37
 38
 39
 40
 41
 42
 43
 44
 45
 46
 47 450
 48
 49
 50
 51
 52
 53
 54
 55
 56
 57
 58
 59
 60
 61
 62
 63
 64
 65

Table 5. Parameters of the Langmuir, Freundlich and Temkin models of adsorption of Acid orange 7 on L and RD at 293, 303 and 313 K

T, K	RD					L					
	K_L , L/g	q_m , mg/g	R^2	ARE	SD	K_L , L/g	q_m , mg/g	R^2	ARE	SD	
293	0.02382	5.5036	0.7780	4.50	0.069	0.003579	22.9358	0.0525	5.91	0.106	
303	0.01203	9.6246	0.2300	7.44	0.114	0.02560	1.7391	0.8366	7.22	0.104	
313	0.01518	6.2735	0.1913	11.32	0.173	0.01973	2.6831	0.3539	17.95	0.24	
	Freundlich model										
	K_p , L/g	n	R^2	ARE	SD	K_F , L/g	n	R^2	ARE	SD	
293	0.1136	0.8447	0.9935	4.17	0.0703	0.07765	0.9581	0.9791	6.04	0.098	
303	0.1043	0.9026	0.9777	6.58	0.108	0.02312	0.6972	0.9967	3.26	0.045	
313	0.0854	0.8872	0.9495	11.02	0.179	0.03134	0.7452	0.9439	14.08	0.192	
	Temkin model										
	A_T , L/g	B	R^2	ARE	SD	A_T , L/g	B	R^2	ARE	SD	
293	0.1136	0.8447	0.9935	28.62	0.474	0.07765	0.9581	0.9791	12.71	0.202	
303	0.1043	0.9026	0.9777	17.11	0.268	0.02312	0.6972	0.9967	14.07	0.232	
313	0.0854	0.8872	0.9495	20.06	0.354	0.03134	0.7452	0.9439	5.11	0.074	

451 The van't Hoff plots of $\ln K_c$ as a function of the reciprocal of the experiment temperatures
1
2
3 452 (293 K, 303 K and 313 K) are presented in Fig. 5 for L and RD. The obtained values of the
4
5 453 change of enthalpy (ΔH^0) and entropy (ΔS^0), calculated from the slopes and intercepts of the
6
7 454 straight lines of the plots respectively, as well as, the values of the free energy change (ΔG^0),
8
9
10 455 calculated according to equation 3, are presented in Table 6. The calculated thermodynamic
11
12 456 parameters were similar for both adsorbents. The calculation suggested that negative values
13
14 457 were observed for ΔG^0 and positive values for ΔH^0 and ΔS^0 at all experimental temperatures
15
16
17 458 for Acid orange 7 adsorption using L and RD by-products. Similar results were published for
18
19 459 adsorption of Acid orange-7 using canola waste [37] and aluminum oxide nanoparticles [44].
20
21
22 460 The negative values of ΔG^0 for both adsorbents implies that the adsorption processes were
23
24 461 spontaneous and feasible [31]. Generally, the adsorption process could be due to physical
25
26 462 phenomenon and chemical interactions. In our case, the observed values ~~decrease~~ of ΔG^0
27
28
29 463 were from -18,000 to -21,000 J/mol, which suggests that the type of interactions between L
30
31 464 and RD and Acid orange 7 was mainly physical and hence physical adsorption occurred. The
32
33
34 465 absolute values of ΔG^0 increased slightly with the temperature rise, which confirmed the
35
36 466 weak temperature's effect on the adsorption of the dye on the L and RD. The positive values
37
38
39 467 of ΔH^0 confirmed that the adsorption processes were endothermic for both by-products which
40
41 468 suggest a lower value of the required amount of heat characterizing the phenomenon of
42
43
44 469 physical sorption. Positive values of ΔS^0 suggested an affinity between the adsorbents and
45
46 470 the azo dye Acid orange 7 and assumed increased randomness at the solid/solution surface of
47
48
49 471 interaction with several structural changes in the adsorbent and the adsorbate.
50
51
52
53
54
55
56
57
58
59
60
61
62
63
64
65

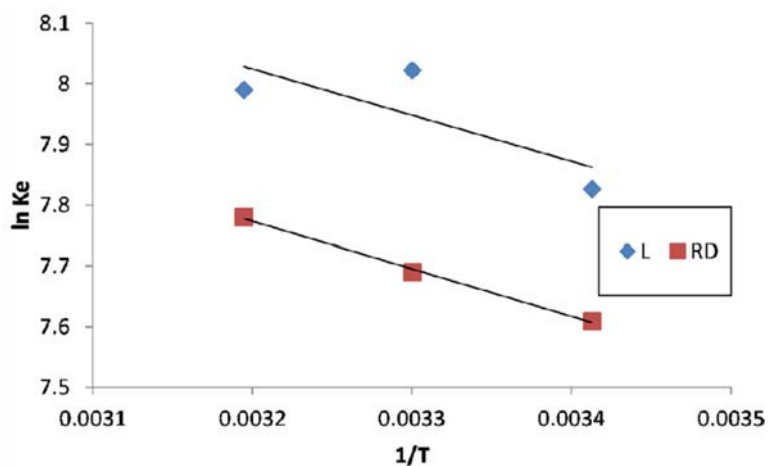


Fig. 5 Graphical representation of $\ln K_e$ versus $1/T$ of the adsorption of Acid orange 7 on L and RD by-products

Table 6. Thermodynamic parameters of adsorption of Acid orange 7 on L and RD residues

	Temperature, K	ΔG^0 , J/mol	ΔH^0 , J/mol	ΔS^0 , J/(mol.K)
	293	-18536		
RD	303	-19373	6504	85
	313	-20246		
	293	-19153		
L	303	-20023	6333	87
	313	-20893		

3.4. Valorization of the spent adsorbents after adsorption of Acid orange 7

Many studies focused only on the adsorption of organic pollutants or heavy metals using agricultural or food by-products (or products derived on their basis) including studies on the kinetics, different factors affecting the adsorption, different adsorbents, etc. In general, it is difficult to dispose of the spent adsorbents directly in the surrounding environment due to the presence of substances that pose environmental risks. Regeneration of the adsorbents is most

1 484 often proposed solution but again the problem with safely handling the washings arises. The
2 485 metabolic activity of different higher fungi and their immense capacity to grow and degrade
3
4 486 different natural and synthetic substrates could support the conversion of these post-
5
6
7 487 adsorption residues into value added products with low ecological footprints. Angelova et al.
8
9
10 488 [20] demonstrated recently that lignocellulose compounds, together with the non-cellulosic
11
12 489 polysaccharides and uronic acids polymers of steam distilled lavender straw and hexane
13
14 490 extracted rose flowers were essential prerequisite for vegetative growth of Basidiomycetes
15
16
17 491 fungi. The above chemical compounds stimulated mycelium net formation and supported the
18
19 492 full lignocellulose substrates colonization that at the end yielded innovative mycelium-based
20
21
22 493 materials with desirable properties.
23
24 494 *G. resinaceum* was chosen not only because of the strain's ability to grow well on different
25
26 495 lignocellulose, but also it's potential to degrade synthetic dyes. *G. resinaceum* belongs to
27
28 496 white-rot fungi (*Basidiomycota* phylum, order *Polyporales*). Due to their ability to produce
29
30 497 extracellular lignin-degrading enzymes (lignin peroxidases, manganese peroxidases and
31
32 498 laccases) in submerged or solid-state cultivation conditions, white-rot fungi have their
33
34 499 advantages in mycoremediation processes for degradation of insoluble chemicals and
35
36
37 500 hazardous environmental pollutants [45, 46]. In many studies focused on decolorization of
38
39 501 synthetic dyes the "key players" are white-rot fungi such as *Trametes versicolor*, *Pleurotus*
40
41
42 502 *ostreatus*, *Ganoderma spp.*, etc. [22, 24, 25, 47].
43
44
45 503 In the present study solid-state cultivations of *G. resinaceum* GA1M using L and RD post-
46
47 504 adsorption residues as feeding substrates were conducted. The twenty-days cultivations,
48
49
50 505 comprising of several stages, resulted in homogenous mycelium-based bio-composites with a
51
52
53 506 desired morphology (Fig. 6). Both obtained materials demonstrated acceptable
54
55
56 507 conformational stability and had velvety tactile surfaces that was the result of well-developed
57
58 508 aerial mycelium and dense hypha networks. These characteristics are of important
59
60
61
62
63
64
65

509 significance for the physical and mechanical properties of these mycelium-based bio-
510 composites which in turn determine the application of the developed biomaterials [20].
511 The obtained mycelium-based bio-composites were analyzed for residual Acid orange 7. The
512 initial concentration of Acid orange 7 in spent adsorbents was in the 1.2-1.3 mg/g adsorbent
513 range. After the fungal growth, transformation and degradation of the lignocellulosic matrix,
514 metabolization of Acid orange 7 also occurred and the dye was not detected in either
515 mycelium-based materials.
516 The azo bond in the azo dyes is the main reason for their persistency since it is non-
517 biodegradable under aerobic conditions. As a member of the Basidiomycetes, *G. resinaceum*
518 possess a ligninolytic enzyme system with very broad substrate specificity which can break
519 the recalcitrant azo bond. It is well known that degradation is not always equal to
520 detoxification, but the Basidiomycetes representatives are able to decolorize and detoxify
521 synthetic dyes and their metabolites. The enzymes that are most extensively used
522 (dependently and independently) in the synthetic dyes' degradation are laccases, lignin
523 peroxidases and manganese peroxidases [21].

524



525

526 **Fig. 6** Mycelium-based biocomposites produced from the L and RD residues resulted from
527 the adsorption of Acid orange 7

528

1 529 The Basidiomycetes *G. resinaceum* proved to be effective in removing the dye Acid orange 7
2 530 during solid-state cultivation on post-adsorption L and RD residues and simultaneously
3
4 531 leading to innovative mycelium-based bio-composites. This approach is consistent with *zero*
5
6 532 *waste* trends which will benefit overall environmental sustainability. Further research is
7
8
9 533 needed to analyze physico-mechanical properties of the produced biomaterials and identify
10
11
12 534 potential applications.
13

14 535

17 536 4. Conclusions

18
19 537

20
21
22 538 The present study focused on decontamination and removal of azo dye Acid orange 7 from
23
24 539 aqueous solutions by combined treatment using industrial rose and lavender solid by-products
25
26 540 as adsorbents and further degradation of the post-adsorption plant biomass by higher fungi
27
28 541 resulting in production of mycelium-based biocomposites. The results suggested that more
29
30
31 542 than 87% of the colorant was removed by the RD adsorbent and around 82% by L residue for
32
33
34 543 one hour at 293 K. The highest adsorption capacity was demonstrated by both adsorbents
35
36 544 with the highest initial concentration of 100 mg/L of the azo dye. The effectiveness of the
37
38
39 545 adsorption increased decreasing the pH medium: for L at pH 1.5 the removal was 1.975 ± 0.08
40
41 546 mg/g (98.75%) and for RD at pH 3.5 was 1.975 ± 0.08 (98.75%). The infrared spectroscopy
42
43
44 547 analyses revealed that around $1500-1560 \text{ cm}^{-1}$ a new peak at 1540 cm^{-1} (for RD post-
45
46 548 adsorption residue) and 1541 cm^{-1} (for L post-adsorption residue) appeared. These bands are
47
48
49 549 due to the aromatic ring stretching vibrations from the aromatic moieties of Acid orange 7
50
51 550 suggesting successful adsorption of the dye onto the surface of the RD and L by-products.
52
53 551 The adsorption of the azo dye was evaluated by Langmuir, Freundlich, and Temkin isotherm
54
55
56 552 models and it was found that the Freundlich equation best described the adsorption of Acid
57
58 553 orange 7 using RD and L by-products. The coefficient n in the Freundlich equation connected
59
60
61
62
63
64
65

554 to adsorption intensity is practically not influenced by the temperature and the type of the
1
2 555 adsorbent. The values of the coefficient K_F showed higher adsorption capacity for RD
3
4
5 556 compared with L's capacity, at the three temperatures studied. Negative values were observed
6
7 557 for ΔG^0 at all experimental temperatures implying that the adsorption processes were
8
9
10 558 spontaneous. The observed decrease of ΔG^0 (ranging from -18,000 to -21,000 J/mol) suggests
11
12 559 mainly physical adsorption occurred. The post-adsorption L and RD residues were then
13
14 560 subjected to solid state cultivation using *G. resinaceum* GA1M. As a result, new
15
16
17 561 biodegradable materials were obtained and the analyses demonstrated that Acid orange 7 was
18
19 562 not found in the resulted mycelium-based biocomposites. Consequently, three main results
20
21
22 563 were achieved: first, RD and L industrial by-products were successfully applied for
23
24 564 adsorption and removal of Acid orange 7 (valorization of rose and lavender essential oil by-
25
26 565 products); second, by solid state cultivation of the post-adsorption L and RD residues Acid
27
28
29 566 orange 7 was degraded by *G. resinaceum* GA1M; and third, new mycelium-based
30
31 567 biodegradable composites with promising application in construction and art were produced.
32
33

34 568

35
36 569 'Statements and Declarations'

37
38
39 570

40
41 571 Funding

42
43
44 572 This work was supported by the Ministry of Education and Science of Bulgaria (Bulgarian
45
46 573 National Science Fund) [Grant Number: KII-06-Austria/4 13/08/2021] and the Federal
47
48
49 574 Ministry of Education, Science and Research (BMBWF) through Austria's Agency for
50
51 575 Education and Internationalization (OeAD) [Grant Number: Africa UNINET P056; BG
52
53 576 01/2021].
54

55
56 577

57
58 578 Competing Interests
59
60
61
62
63
64
65

1
2
3 579 The authors have no competing interests to declare that are relevant to the content of this
4
5 580 article.
6
7 581
8
9 582 Author Contributions
10 583 Data curation: [Gergana Marovska], [Nikolay Menkov], [Mariya Dushkova], [Galena
11
12 584 Angelova], [Mariya Brazkova], [Anton Slavov]
13
14 585 Investigation: [Gergana Marovska], [Nikolay Menkov], [Mariya Dushkova], [Galena
15
16 586 Angelova], [Mariya Brazkova], [Anton Slavov]
17
18 587 Methodology: [Nikolay Menkov], [Anton Slavov], [Galena Angelova]
19
20 588 Formal analysis: [Nikolay Menkov], [Anton Slavov], [Galena Angelova], [Gergana
21
22 589 Marovska]
23
24 590 Writing- Reviewing and Editing: [Anton Slavov], [Nikolay Menkov], [Hendrik Brink],
25
26 591 [Galena Angelova], [Mariya Dushkova], [Nils Haneklaus]
27
28 592 Conceptualization: [Anton Slavov], [Nikolay Menkov], [Galena Angelova], [Gergana
29
30 593 Marovska]
31
32 594 Funding acquisition: [Anton Slavov], [Nils Haneklaus]
33
34 595 Project administration: [Anton Slavov], [Nils Haneklaus]
35
36 596 Availability of data and materials
37
38 597 All data generated or analyzed during this study are included in this published article.
39
40 598
41
42 599 Compliance with Ethical Standards
43
44 600
45
46 601 Ethical approval
47
48
49
50
51
52
53
54
55
56
57
58
59
60
61
62
63
64
65

602 This article does not contain any studies with human participants. All applicable
1
2 603 international, national, and/or institutional guidelines for the care and use of animals were
3
4
5 604 followed.
6
7 605 Informed consent
8
9
10 606 Not applicable.
11
12 607 Consent to participate
13
14 608 Not applicable.
15
16 609 Consent for publication
17
18 610 Not applicable.
19
20
21 611
22
23
24 612 5. References
25
26 613
27
28 614 1. Benkhaya S, M'rabet S, El Harfi A (2020) Classifications, properties, recent synthesis and
29
30 615 applications of azo dyes. Heliyon 6:e03271. <https://doi.org/10.1016/j.heliyon.2020.e03271>
31
32
33 616 2. Wakelyn PJ (2007) Health and safety issues in cotton production and processing. In:
34
35 617 Gordon S, Hsieh YL (ed) Cotton, 1st edn. Woodhead Publishing Limited, Sawston, pp 460-
36
37 618 483. <https://doi.org/10.1533/9781845692483.3.460>
38
39
40 619 3. Elgarahy AM, Maged A, Elwakeel KZ, El-Gohary F, El-Qelish M (2023) Tuning
41
42 620 cationic/anionic dyes sorption from aqueous solution onto green algal biomass for
43
44 621 biohydrogen production. Environ Res 216:114522.
45
46
47 622 <https://doi.org/10.1016/j.envres.2022.114522>
48
49
50 623 4. Du R, Cao H, Wang G, Dou K, Tsidaeva N, Wang W (2022) PVP modified rGO/CoFe₂O₄
51
52 624 magnetic adsorbents with a unique sandwich structure and superior adsorption performance
53
54 625 for anionic and cationic dyes. Separ Purif Technol 286:120484.
55
56
57 626 <https://doi.org/10.1016/j.seppur.2022.120484>
58
59
60
61
62
63
64
65

- 627 5. Crettaz S, Kämpfer P., Brüscheiler BJ, Nussbaumer S, Deflorin O (2020) Survey on
1
2 628 hazardous non-regulated aromatic amines as cleavage products of azo dyes found in clothing
3
4
5 629 textiles on the Swiss market. *J Consum Prot Food Safety* 15:49-61.
6
7 630 <https://doi.org/10.1007/s00003-019-01245-1>
8
9
10 631 6. Brüscheiler BJ, Merlot C (2017) Azo dyes in clothing textiles can be cleaved into a series
11
12 632 of mutagenic aromatic amines which are not regulated yet. *Regul Toxicol Pharmacol* 88:214-
13
14 633 226. <https://doi.org/10.1016/j.yrtph.2017.06.012>
15
16
17 634 7. Kaur N, Kaushal J (2022) Screening the six plant species for phytoremediation of synthetic
18
19 635 textile dye waste water. *Mater Today: Proc* 71:232-238.
20
21
22 636 <https://doi.org/10.1016/j.matpr.2022.08.512>
23
24 637 8. Jankowska K, Su Z, Zdarta J, Jesionowski T, Pinelo M (2022) Synergistic action of laccase
25
26 638 treatment and membrane filtration during removal of azo dyes in an enzymatic membrane
27
28 639 reactor upgraded with electrospun fibers. *J Hazard Mater* 435:129071.
29
30
31 640 <https://doi.org/10.1016/j.jhazmat.2022.129071>
32
33
34 641 9. Khan N, Ahmad A, Sharma V, Saha AK, Pandey A, Bhargava PC (2022) An integrative
35
36 642 study for efficient removal of hazardous azo dye using microbe-immobilized cow dung
37
38 643 biochar in a continuous packed bed reactor. *Renew Energy* 200:1589-1601.
39
40
41 644 <https://doi.org/10.1016/j.renene.2022.10.016>
42
43
44 645 10. Nurhayati E, Bagastyo AY, Hartatik DD, Direstiyani LC (2020) The enhancement of
45
46 646 biodegradability index of mature landfill leachate by electrochemical oxidation process using
47
48 647 boron-doped diamond and dimensionally stable anode. *Res Chem Intermed* 46:4811-4822.
49
50
51 648 <https://doi.org/10.1016/j.molliq.2019.110928>
52
53
54 649 11. Tran HT, Lin C, Bui XT, Nguyen MK, Cao NDT, Mukhtar H, Hoang HG, Varjani S, Ngo
55
56 650 HH, Nghiem LD (2022) Phthalates in the environment: characteristics, fate and transport, and
57
58
59
60
61
62
63
64
65

- 651 advanced wastewater treatment technologies. *Bioresour Technol* 344:126249.
652 <https://doi.org/10.1016/j.biortech.2021.126249>
- 653 12. Xie S, Li M, Liao Y, Qin Q, Sun S, Tan Y (2021) In-situ preparation of biochar loaded
654 particle electrode and its application in the electrochemical degradation of 4-chlorophenol in
655 wastewater. *Chemosphere* 273:128506. <https://doi.org/10.1016/j.chemosphere.2020.128506>
- 656 13. Taheri M, Fallah N, Nasernejad B (2022) Which treatment procedure among
657 electrocoagulation, biological, adsorption, and bio-adsorption processes performs best in azo
658 dyes removal? *Water Resour Ind* 28:100191. <https://doi.org/10.1016/j.wri.2022.100191>
- 659 14. Boulahbal M, Malouki MA, Canle M, Redouane-Salah Z, Devanesan S, AlSalhi MS,
660 Berkani M (2022) Removal of the industrial azo dye crystal violet using a natural clay:
661 Characterization, kinetic modeling, and RSM optimization. *Chemosphere* 306:135516.
662 <https://doi.org/10.1016/j.chemosphere.2022.135516>
- 663 15. Mittal A, Gupta VK, Malviya A, Mittal J (2008) Process development for the batch and
664 bulk removal and recovery of a hazardous, water-soluble azo dye (metanil yellow) by
665 adsorption over waste materials (bottom ash and de-oiled soya). *J Hazard Mater* 151:821-832.
666 <https://doi.org/10.1016/j.jhazmat.2007.06.059>
- 667 16. Putro JN, Santoso SP, Soetaredjo FE, Ismadji S, Ju YH (2019) Nanocrystalline cellulose
668 from waste paper: Adsorbent for azo dyes removal. *Environ Nanotechnol Monit Manag*
669 12:100260. <https://doi.org/10.1016/j.enmm.2019.100260>
- 670 17. Slavov A, Vasileva I, Stefanov L, Stoyanova A (2017) Valorization of wastes from the
671 rose oil industry. *Rev Environ Sci Biotechnol* 16:309-325. [https://doi.org/10.1007/s11157-
672 017-9430-5](https://doi.org/10.1007/s11157-017-9430-5)
- 673 18. Echavarria-Alvarez AM, Hormaza-Anaguano A (2014) Flower wastes as a low-cost
674 adsorbent for the removal of acid blue 9. *Dyna* 81:132-138.
675 <https://doi.org/10.15446/dyna.v81n185.37234>

676 19. Rabbani D, Mahmoudkashi N, Mehdizad F, Shaterian M (2016) Green approach to
677 wastewater treatment by application of *Rosa damascena* waste as nano-biosorbent. J Environ
678 Sci Technol 9:121-130. <https://doi.org/10.3923/jest.2016.121.130>

679 20. Angelova G, Brazkova M, Stefanova P, Blazheva D, Vladev V, Petkova N, Slavov A,
680 Denev P, Karashanova D, Zaharieva R, Enev A, Krastanov A (2021) Waste rose flower and
681 lavender straw biomass – An innovative lignocellulose feedstock for mycelium bio-materials
682 development using newly isolated *Ganoderma resinaceum* GA1M. J Fungi 7:866.
683 <https://doi.org/10.3390/jof7100866>

684 21. Brazkova M, Koleva R, Angelova G, Yemendzhiev H (2022) Ligninolytic enzymes in
685 *Basidiomycetes* and their application in xenobiotics degradation. BIO Web Conf 45:02009.
686 <https://doi.org/10.1051/bioconf/20224502009>

687 22. Eichlerová I, Baldrian P (2020) Ligninolytic enzyme production and decolorization
688 capacity of synthetic dyes by saprotrophic white rot, brown rot, and litter decomposing
689 *Basidiomycetes*. J Fungi 6:301. <https://doi.org/10.3390/jof6040301>

690 23. Liu J, Sun S, Han Y, Meng J, Chen Y, Yu H, Zhang X, Ma F (2021) Lignin waste as co-
691 substrate on decolorization of azo dyes by *Ganoderma lucidum*. J Taiwan Inst Chem Eng
692 122:85-92. <https://doi.org/10.1016/j.jtice.2021.04.039>

693 24. Martínez-Sánchez J, Membrillo-Venegas I, Martínez-Trujillo A, García-Rivero A (2018)
694 Decolorization of reactive black 5 by immobilized *Trametes versicolor*. Rev Mex Ing Quim
695 17:107-121. <https://doi.org/10.24275/uam/izt/dcbi/revmexingquim/2018v17n1/Martinez>

696 25. Rainert KT, Nunes HCA, Gonçalves MJ, Helm CV, Tavares LBB (2021) Decolorization
697 of the synthetic dye Remazol Brilliant Blue Reactive (RBBR) by *Ganoderma lucidum* on bio-
698 adsorbent of the solid bleached sulfite paperboard coated with polyethylene terephthalate. J
699 Environ Chem Eng 9:104990. <https://doi.org/10.1016/j.jece.2020.104990>

- 1
2
3
4
5
6
7
8
9
10
11
12
13
14
15
16
17
18
19
20
21
22
23
24
25
26
27
28
29
30
31
32
33
34
35
36
37
38
39
40
41
42
43
44
45
46
47
48
49
50
51
52
53
54
55
56
57
58
59
60
61
62
63
64
65
- 700 26. Günay A, Arslankaya E, Tosun I (2007) Lead removal from aqueous solution by natural
701 and pretreated clinoptilolite: Adsorption equilibrium and kinetics. J Hazard Mater 146:362-
702 371. <https://doi.org/10.1016/j.jhazmat.2006.12.034>
- 703 27. Shikuku VO, Kowenje CO, Kengara FO (2018) Errors in parameters estimation using
704 linearized adsorption isotherms: Sulfadimethoxine adsorption onto kaolinite clay. Chem Sci
705 Int J 23:1-6. <https://doi.org/10.9734/CSJI/2018/44087>
- 706 28. Elmorsi T (2011) Equilibrium isotherms and kinetic studies of removal of methylene blue
707 dye by adsorption onto miswak leaves as a natural adsorbent. J Environ Prot 2:817-827.
708 <https://doi.org/10.4236/jep.2011.26093>
- 709 29. Olasehinde EF, Abegunde SM, Adebayo MA (2020) Adsorption isotherms, kinetics and
710 thermodynamic studies of methylene blue dye removal using *Raphia taedigera* seed activated
711 carbon. Casp J Environ Sci 18:329-344. <https://doi.org/10.22124/cjes.2020.4279>
- 712 30. Khan AA, Singh RP (1987) Adsorption thermodynamics of carbofuran on Sn (IV)
713 arsenosilicate in H⁺, Na⁺ and Ca²⁺ forms. Colloids Surf 24:33-42.
714 [https://doi.org/10.1016/0166-6622\(87\)80259-7](https://doi.org/10.1016/0166-6622(87)80259-7)
- 715 31. Kodrić M, Reka A, Dimić Č, Tarbuk A, Đorđević D (2020) Thermodynamic investigation
716 of disperse dyes sorption on polyester fibers. Adv Technol 9:41-47.
717 <https://doi.org/10.5937/savteh2002041K>
- 718 32. Kul AR, Aldemir A, Alkan S, Elik H, Çalışkan M (2019) Adsorption of Basic Blue 41
719 using *Juniperus excelsa*: Isotherm, kinetics and thermodynamics studies. Environ Res
720 Technol 2:112-121. <https://doi.org/10.35208/ert.568992>
- 721 33. Hamzeh Y, Ashori A, Azadeh E, Abdulkhani A (2012) Removal of Acid Orange 7 and
722 Remazol Black 5 reactive dyes from aqueous solutions using a novel biosorbent. Mater Sci
723 Eng C 32:1394-1400. <https://doi.org/10.1016/j.msec.2012.04.015c>

- 724 34. Marovska G, Vasileva I, Petkova N, Ognyanov M, Gandova V, Stoyanova A,
1
2 725 Merdzhyanov P, Simitchiev A, Slavov A (2022) Lavender (*Lavandula angustifolia* Mill.)
3
4 726 industrial by-products as a source of polysaccharides. *Ind Crops Prod* 188(B):115678.
5
6
7 727 <https://doi.org/10.1016/j.indcrop.2022.115678>
8
9
10 728 35. Wu Y, Hu Y, Xie ZW, Feng SX, Li B, Mi XM (2011) Characterization of biosorption
11
12 729 process of acid orange 7 on waste brewery's yeast. *Appl Biochem Biotechnol* 163:882-894.
13
14 730 <https://doi.org/10.1007/s12010-010-9092-z>
15
16
17 731 36. Pelosi BT, Lima LKS, Vieira MGA (2013) Acid orange 7 dye biosorption by *Salvinia*
18
19 732 *natans* biomass. *Chem Eng Trans* 32:1051-1056. <https://doi.org/10.3303/CET1332176>
20
21
22 733 37. Balarak D, Abasizadeh H, Yang JK, Shim MJ, Lee SM (2020) Biosorption of Acid Orange
23
24 734 7 (AO7) dye by canola waste: equilibrium, kinetic and thermodynamics studies. *Desalin Water*
25
26 735 *Treat* 190:331-339. <https://doi.org/10.5004/dwt.2020.25665>
27
28
29 736 38. Sillanpää M, Mahvi AH, Balarak D, Khatibi AD (2021) Adsorption of Acid orange 7
30
31 737 dyes from aqueous solution using Polypyrrole/nanosilica composite: Experimental and
32
33 738 modelling. *Int J Environ Anal Chem* 103:212-229.
34
35 739 <https://doi.org/10.1080/03067319.2020.1855338>
36
37
38 740 39. Gupta VK, Mittal A, Gajbe V, Mittal J (2006) Removal and recovery of the hazardous azo
39
40 741 dye Acid orange 7 through adsorption over waste materials: Bottom ash and de-oiled soya. *Ind*
41
42 742 *Eng Chem Res* 45:1446-1453. <https://doi.org/10.1021/ie051111f>
43
44
45 743 40. Izadyar S, Rahimi M (2007) Use of beech wood sawdust for adsorption of textile dyes. *Pak*
46
47 744 *J Biol Sci* 10:287-293. <https://doi.org/10.3923/pjbs.2007.287.293>
48
49
50 745 41. Coates J (2006) Interpretation of infrared spectra, a practical approach. In: Meyers R (ed)
51
52 746 *Encyclopedia of Analytical Chemistry*. Wiley, Chichester, pp 1-23.
53
54 747 <https://doi.org/10.1002/9780470027318.a5606>
55
56
57
58
59
60
61
62
63
64
65

- 748 42. Lim CK, Bay HH, Aris A, Majid ZA, Ibrahim Z (2013) Biosorption and biodegradation
1
2 749 of Acid Orange 7 by *Enterococcus faecalis* strain ZL: optimization by response surface
3
4
5 750 methodological approach. *Environ Sci Pollut Res Int* 20:5056-5066.
6
7 751 <https://doi.org/10.1007/s11356-013-1476-5>
8
9
10 752 43. Ertugay N, Mallkoc E (2014) Adsorption isotherm, kinetic, and thermodynamic studies
11
12 753 for methylene blue from aqueous solution by needles of *Pinus Sylvestris* L. *Pol J Environ*
13
14 754 *Stud* 23(6):1995-2006.
15
16
17 755 44. Khosla E, Kaur S, Dave PN (2013) Mechanistic study of adsorption of Acid Orange-7
18
19 756 over aluminum oxide nanoparticles. *J Eng* 2013: 593534.
20
21
22 757 <https://doi.org/10.1155/2013/593534>45. Ngadin AA, Taghavi E, Eaton T (2022) The
23
24 758 development of white-rot fungi as a mycoremediation product. In: Shukla AC (ed) *Applied*
25
26 759 *Mycology. Entrepreneurship with fungi*. Springer, Cham, pp 75-94.
27
28
29 760 https://doi.org/10.1007/978-3-030-90649-8_3
30
31
32 761 46. Sosnicka A, Kózka B, Makarova K, Giebułtowiec J, Klimaszewska M, Turło J (2022)
33
34 762 Optimization of white-rot fungi mycelial culture components for bioremediation of
35
36 763 pharmaceutical-derived pollutants. *Water* 14:1374. <https://doi.org/10.3390/w14091374>
37
38
39 764 47. Krastanov A, Koleva R, Alexieva Z, Stoilova I (2013) Decolorization of industrial dyes by
40
41 765 immobilized mycelia of *Trametes Versicolor*. *Biotechnol Biotechnol Equip* 27:4263-4268.
42
43
44 766 <https://doi.org/10.5504/BBEQ.2013.0096>
45
46
47
48
49
50
51
52
53
54
55
56
57
58
59
60
61
62
63
64
65

